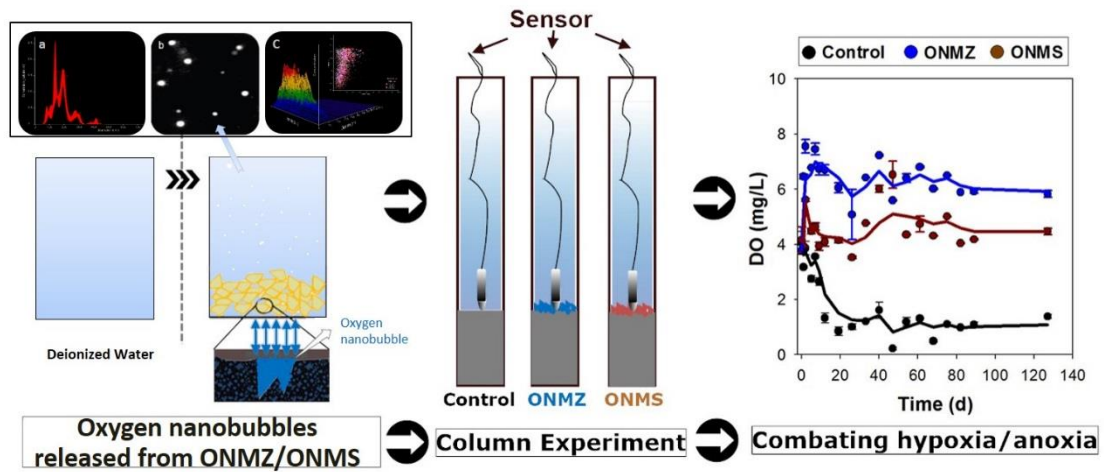# Graphic Abstract

Highlights

- Oxygen nanobubble is a potentially promising technique to mitigate hypoxia/anoxia

- Oxygen nanobubble modified zeolite can effectively deliver oxygen to bottom water

- The oxygen-locking surface sediment layer is crucial in reducing sediment anoxia

- Oxygen-locking sediment layer can switch the anoxia sediment from P source to sink

Combating hypoxia/anoxia at sediment-water interfaces: a preliminary study of oxygen nanobubble modified clay materials

Honggang Zhang[1], Tao Lyu[2], Lei Bi[1], Grant Tempero[3], David P. Hamilton[3], Gang Pan[*1,2]

[1]*Research Center for Eco-Environmental Sciences, Chinese Academy of Sciences, Beijing 100085, China*

[2]*School of Animal, Rural and Environmental Sciences, Nottingham Trent University, Brackenhurst Campus, NG250QF, UK*

[3]*School of Science, University of Waikato, Private Bag 3105, Hamilton 3240, New Zealand*

[*]Corresponding author: gpan@rcees.ac.cn (GP)

Abstract

Combating hypoxia/anoxia is an increasingly common need for restoring natural waters suffering from eutrophication. The oxygen nanobubble modified natural particles were investigated for mitigating hypoxia/anoxia at sediment-water interfaces (SWI) in a simulated column experiment. By adding oxygen nanobubble modified zeolites (ONMZ) and local soils (ONMS), the oxygen nanobubble concentrations (10^5-10^7 particles/mL) were several orders of magnitude higher in the water than the original water solution (10^4 particles/mL) within 24 hours. In the column experiment, an oxygen-locking surface sediment layer were formed after capping with ONMZ and ONMS particles. The synergy of diffusion of oxygen nanobubbles and retention of oxygen in this layer contributes to both the increase of DO and reversal of hypoxic conditions. The overlaying water maintained significantly higher dissolved oxygen (DO) values (4-7.5 mg/L) over the experimental

period of 127 days in ONMZ and ONMS compared with the control systems (around 1 mg/L).

Moreover, the oxidation-reduction potential (ORP) was reversed from -200 mV to 180-210 mV and

maintained positive values for 89 days in ONMZ systems. In the control systems, ORP was

consistently negative and decreased from -200 mV to -350 mV. The total phosphorus (TP) flux from

sediment to water across SWI was negative in the ONMZ and ONMS treated systems, but positive

in the control system, indicating the sediment could be switched from TP source to sink. The oxygen-

locking capping layer was crucial in preventing oxygen consumption caused by the reduced

substances released from the anoxic sediment. The study outlines a potentially promising technology

for mitigating sediment anoxia and controlling nutrients release from sediments, which could

contribute significantly to addressing eutrophication and ecological restoration.

1. Introduction

Hypoxia/anoxia is a global threat to aquatic ecosystems, often inducing "dead zones" at the

sediment-water interface (SWI) (Diaz and Rosenberg, 2008; Feist et al., 2016; Stramma et al., 2008).

In the dead zones, sediment release rates may be accelerated for many constituents, including

phosphorus, nitrogen, iron, manganese, methyl-mercury and hydrogen sulfide (Beutel et al., 2008;

De Vittor et al., 2016; Gantzer et al., 2009; Testa and Kemp, 2012; Zhu et al., 2013). Among the

released substances, phosphorus and nitrogen can lead to eutrophication, which is often associated

with harmful algal blooms (Funkey et al., 2014). Moreover, the hypoxic/anoxic condition can be

exacerbated by the additional oxygen demand from the mineralization of dead algal biomass (Diaz

and Rosenberg, 2008; Testa and Kemp, 2012). Thus, mitigation of hypoxia/anoxia at the SWI is crucial for both water quality improvement and eutrophication control.

Current efforts de-signed to replenish benthic dissolved oxygen (DO) and remove the anoxic environment are often based on the directly injecting either air (aeration) (Henares et al., 2015), or oxygen gas (oxygenation) (Bierlein et al., 2017) sometimes using oxygen-supersaturated water (Forth et al., 2015) into the hypoxic region near the SWI. Although these techniques have been reported to be effective to some extent, they are still limited by high cost and efficiency at large scale (Bormans et al., 2016). Additionally, gas or water pumped into the SWI region may disturb the settled sediment and induce internal releases of nutrients and other contaminants to the water column, as well as potentially leading to additional oxygen consumption and increase hypoxia (Bierlein et al., 2017). The pump system also needs to be continuously operated to maintain the oxygen supply to the SWI, otherwise DO may be rapidly consumed, leading to rapid return of anoxia (Bryant et al., 2010). In the Baltic Sea, where hypoxic waters have expanded in area from 5,000 to $> 60,000$ km^2 in the last century (Carstensen et al., 2014), enhanced ventilation of deep waters through additional input of oxygenated surface water has been suggested (Conley et al., 2009). However, this method will require $>$ 30 years to take effect and may cause a drastic change in stratification and alteration of the biodiversity (Funkey et al., 2014). Ventilation by pumping oxygen-rich water downward to alleviate hypoxia in the Baltic Sea is estimated to require more than 100 pump stations (0.6 MW each) at a cost of around 20,000 million Euros (Stigebrandt and Gustafsson, 2007). Therefore, developing a more cost-effective and sustainable technique for hypoxia/anoxia mitigation in bottom waters and at the SWI is vitally important.

62   Oxygen nanobubbles have attracted increasing attention in recent years due to the

63   characteristics of high gas solubility and long lifetime of oxygen in the liquid (Ebina et al., 2013;

64   Peng et al., 2015). As opposed to oxygen gas (Cavalli et al., 2009), nano-scale oxygen bubbles could

65   slowly diffuse oxygen into the surrounding water phase and last more than 70 days when diameter is

66   <200 nm (Ebina et al., 2013). The oxygen nanobubble technique has already been widely used in

67   medicine (Cai et al., 2015), physiology (Ebina et al., 2013) and water treatment (Agarwal et al., 2011).

68   However, a cost-effective method to deliver the oxygen nanobubble into SWI for hypoxia/anoxia

69   mitigation remains a bottleneck. It was recently reported that oxygen nanobubbles can be generated

70   and persist at solid particle-water interfaces (i.e., surface nanobubbles) (Pan et al., 2016; Wang et al.,

71   2016; Yang et al., 2013). The presence of oxygen nanobubbles has been proven and quantified at the

72   rough and irregular surfaces of clay particles (Pan et al., 2016). It is a means to increase total oxygen

73   content in a suspension by adding clay particles loading with oxygen nanobubbles (Pan and Yang,

74   2012; Pan et al., 2011). Sedimentation of a carrier loaded with oxygen nanobubbles due to the gravity

75   effect provides a mechanism to alter the hypoxia/anoxia near the SWI but has not been investigated

76   systematically.

77   Many geo-engineering methods, such as adding phosphorus-adsorbing materials, have been

78   demonstrated to significantly contribute to remediating eutrophication control and contributing to

79   lake restoration (Huser et al., 2016; Noyma et al., 2016; Spears et al., 2014; Waajen et al., 2016).

80   However, the sinking materials cover the sediment and their effect on redox potential at the SWI may

81   be temporary (Pan et al., 2012). Additionally, most of the adsorbing materials, e.g., metal salts and

82   Phoslock®, are synthesized artificially and may have potential side-effects on the environment.

83   Natural sediments entering lakes through weathering and runoff, have high microporous surface area

84   (Pan et al., 2013). These natural particles have potentially as oxygen nanobubble carriers to deliver

85   oxygen to the SWI. However, no previous study has applied such technology and there is little

86   knowledge about the effects of oxygen nanobubbles on the oxygen conditions, redox potential and

87   nutrient fluxes at the SWI.

88   The objective of this study is to investigate for the first time the efficacy and sustainability of a

89   surface oxygen nanobubble technique for mitigating hypoxia/anoxia and its effect on nutrient fluxes

90   across the SWI. Local soil and natural zeolite were selected as the oxygen nanobubble carriers in the

91   experiment. After oxygen nanobubble modified zeolite (ONMZ) or oxygen nanobubble modified

92   soils (ONMS) were applied in simulated eutrophic water-sediment systems in the laboratory columns,

93   oxygen levels in the overlying water and redox potential at SWI were monitored. Nutrient

94   concentrations, including total phosphorus (TP), total nitrogen (TN), ammonium (NH_4^+-N), nitrate

95   (NO_3^--N), and nitrite (NO_2^--N), were measured in the overlying water and nutrient fluxes across the

96   SWI were calculated.

2. Materials and methods

2.1 Preparation of oxygen nanobubble modified materials

99   Natural zeolite and local soil were selected as the carrier materials to investigate the effect of

100   surface oxygen nanobubble technology on hypoxia/anoxia mitigation at the SWI. Zeolite with particle

101   size of 1-2 mm was purchased from Yongjia Natural Minerals Ltd., Hebei, China. Local soil from

102   Lake Ngaroto, Waikato, New Zealand, was sieved through a mesh sieve to remove particles >380 μm.

103   Ngaroto is the largest peat lake in Waikato region, with a surface area of about 108 ha, maximum

104   depth of 4 m and average depth of c. 2 m. Land in the catchment of this lake is mostly used for pastoral

105   grazing. The lake is hypertrophic and has major cyanobacteria harmful algal blooms throughout

106   summer. The specific surface area and micropore size of the natural zeolite and local soil were

107   determined by the Brunauer–Emmett–Teller (BET) method with a Micromeritrics ASAP-2020

108   apparatus (Micromeritics Inc., USA) (Zhang et al., 2014).

109   The zeolite and soil, were washed with deionized water and dried for 10 h at 90 °C. The

110   preparation of oxygen nanobubble modified zeolite (ONMZ) and soil (ONMS) followed a modified

111   method based on exposure to oxygen supersaturating ambient conditions (Pan et al., 2016). Briefly,

112   the materials (zeolite or soil) were placed into a pressure-resistant and airtight container. A vacuum

113   was created to hold pressure to -0.08 to -0.1 MPa for 2 h to remove gas from the micropores of zeolite

114   and soil. Thereafter, pure O_2 (99.99%) was pumped into the container and held at a pressure of 0.12

115   to 0.15 MPa for 4 h to load the O_2. The oxygen nanobubble loading process, including the creation

116   of the vacuum, was repeated three times to achieve supersaturation of O_2 in the particle micropores.

117   **2.2 Nanobubbles analysis**

118   Prior to the column experiment, the release potential of oxygen nanobubbles into water from

119   the modified solid particles was tested via a flask experiment. Twenty grams of the oxygen

120   nanobubble modified zeolite or soil was put into 250 mL flasks with 200 mL deionized water and

121   sealed by gas-permeable sealing film (0.3 µm). Controls consisted of flasks of 250 mL filled with 200

122   mL of deionized water. Each control and treatment flask experiment were conducted in triplicate. To

123   confirm the sequential changes of nanobubble release, size (detection range; 10-1000 nm) and

124   concentration of oxygen nanobubbles, measurements were conducted at 1 min, 6 h and 24 h in a

125   nanoparticle-tracking analysis instrument (NanoSight NS500 & NTA 2.0 Analytical Software,

126　　Malvern Instrument Ltd, Salisbury, UK) at room temperature ($24 \pm 1\,^{\circ}C$).

127　　**2.3 Column experiment**

128　　　　The column experiment was conducted in an indoor laboratory in University of Waikato, New

129　　Zealand, over a total duration of 127 days. Six plexiglass cylinders with identical inner diameter of

130　　12 cm and height of 150 cm were used as incubation columns (Fig. S1**Error! Reference source not**

131　　**found.**). Each column was filled in the bottom 20 cm with the lake sediment and with filtered (mesh

132　　size of 25 μm) lake water (also from Lake Ngaroto) to a height of 120 cm. Each experimental column

133　　was wrapped with black plastic to shield the system from ambient light. The columns included

134　　duplicates of a control, treatment by oxygen nanobubble modified natural zeolite (ONMZ) and

135　　oxygen nanobubble modified local soil (ONMS). The oxidation-reduction potential (ORP) meter

136　　(HANNA, HI2001) was placed lightly on the sediment surface in each column to monitor the change

137　　of ORP at the SWI throughout the experiment. After a 3-day stabilization period, the ONMZ and

138　　ONMS treatment systems were pretreated by flocculation using 3 mg/L chitosan modified soils (Li

139　　and Pan, 2013) following by application of approximately 100 g of ONMZ and ONMS, resulting a 2

140　　cm depth capping layer.

141　　**2.4 Sampling and analysis**

142　　　　During the experiment, overlying water samples (100 mL) from each column were carefully

143　　collected from 5 cm above the sediment using a syringe with a siphon. The collected water samples

144　　were evenly separated into three parts (c.33 mL) which were measured for turbidity and nutrient

145　　concentrations (TP, TN, NH_4^+-N, NO_3^--N, and NO_2^--N). After each sample collection, all columns

146　　were slowly replenished with the original filtered lake water to compensate for the sampling losses.

147   Turbidity was analyzed with portable turbidity meter (HANNA, HI98713). TP was determined using

148   a potassium persulfate digestion-Mo-Sb-Vc colorimetric method, TN using an alkaline potassium

149   persulphate digestion−ultraviolet spectrometer, NH_4^+-N with Nessler's colorimetric, and NO_3^--N and

150   NO_2^--N with ultraviolet colorimetric method with and without cadmium column reduction,

151   respectively (APHA, 1998). The DO was measured using a Yellow Springs Instruments (YSI, Proplus)

152   by carefully putting the meters into the overlying water and holding at 1-2 cm above the SWI. To

153   avoid cross contamination, the meters were carefully cleaned with Milli-Q water and ethanol between

154   measurements. The DO and turbidity were measured simultaneously with ORP from the in-site meters

155   (HANNA, HI2001) at days 0, 1, 2, 5, 7, 9, 12 and then every around 7 days until day 89, although

156   DO was measured until day 127. The concentrations of TP, TN, NH_4^+-N, NO_3^--N, and NO_2^--N were

157   measured at 7-day frequency until 47 days and then monitored every 14 days. The nutrient fluxes

158   were calculated from day 19 in order to minimize the influence caused by suspended substances

159   sedimentation as indicated by relative low turbidity in control. All samples were tested in triplicate

160   for each duplicate column, values were averaged and standard deviations for the samples from the

161   same treatment system.

162   **2.5 Calculation**

163   The monitoring data on nutrient concentrations obtained after day 19 was used to calculate

164   nutrient fluxes at the SWI. The average nutrient flux was calculated according to the following mass

165   balance Equation (1):

166   $$F_n = \frac{[V(c_n - c_m) + \sum_{j=1, i=1}^{n} V_j(c_n - c_i)]}{S \times t} \tag{1}$$

167   Where F_n is the flux on n^{th} sampling day ($mgm^{-2}d^{-1}$), V is the volume of overlying water (L), c_n is the nutrient

168 concentration (mgL^{-1}) on n^{th} sampling day (n>19), c_m is the nutrient concentration (mgL^{-1}) on m^{th} sampling day

169 when turbidity had stabilized in the three columns (i.e., the 19th day in this study), c_i is the nutrient

170 concentration of the compensating water for maintaining the volume of water in the columns (mgL^{-1}

171 ^{1}), V_j is volume of sampling water (L), S is the cross section area of each column (m^2) and t is incubation time

172 (d).

173 **2.6 Statistical Analysis**

174   Sigmaplot software (version 12.5, Sigma, Inc.) and SPSS16.0 (Statistical Program for Social

175 Sciences) were used for plotting and data analyses, respectively. A one-way ANOVA and post hoc

176 Tukey's HSD test were used to compare water quality parameters (DO, ORP and turbidity) and

177 nutrient concentrations between different treatment systems (control, ONMZ and ONMS) at each

178 corresponding sampling point, with differences accepted at a significance level <0.05. To fully

179 understand the effect of surface oxygen nanobubble technology on the hypoxia/anoxia mitigation in

180 the column experiment, principal component analysis (PCA) was used to provide an overview of the

181 system performance using a visualization method to normalize all parameters. PCA was used to

182 identify different performance patterns between control, ONMZ and ONMS treatment systems during

183 from day 19 to day 89 of the experiment. PCA was conducted using all measured parameters,

184 including DO, ORP, turbidity, TP, TN, NH_4^+-N, NO_3^--N and NO_2^--N. The data was standardized (to

185 a Z score with a mean = 0 and S.D. = 1) to ensure that each variable had the same influence in the

186 analysis. Multiple correlation analysis was carried out to assess the relationships between all

187 measured parameters in the column experiment. The data was checked for normality and

188 homogeneity of variance prior to all statistical analysis. If variables were not normally distributed,

189 they were log-transformed.

3. Results

3.1 Release of oxygen nanobubbles from ONMZ and ONMS

In order to verify the release of oxygen nanobubbles from the modified particles, the water solution in the flask experiment after ONMZ and ONMS addition was analyzed in a nanoparticle-tracking analysis instrument to detect the concentration and size of the nanobubbles. The concentrations of nanobubbles were both around 10^7 particles/mL immediately after the addition (1 min) of ONMZ (Fig. 1) and ONMS (Fig. 2) into the water, and approximately 70% of the released nanobubbles were <200 nm in diameter. The concentration of nanobubbles in the water with ONMZ addition was maximal at 24 h (still around 10^7 particles/mL), and the concentration in the water with ONMS addition decreased to 10^5 particles/mL. Nevertheless, the concentrations were clearly elevated compared with the original deionized water, which remained around 10^4 particles/mL (Fig. S2). The peaks in the concentration vs. size graph (Fig. 1) move toward the right direction of the x axis, which indicates that the size of nanobubbles gradually increased along with the culture time in both ONMZ and ONMS (Fig. 2) treated water. The 3D graph shows two distinct nanobubble populations, clearly confirmed by the higher light scattering intensity of the nanobubbles in ONMZ treated water compared to the ONMS treated water.

3.2 DO and ORP dynamics at the sediment-water interfaces

At the beginning of the column experiment, the DO and ORP of the overlying water in all systems were around 4 mg/L (Fig. 3a) and -200 mV (Fig. 3b), respectively. After the oxygen nanobubble modified particles application, DO increased in the first 5 days and reached around 7.5 and 5.5 mg/L in ONMZ and ONMS systems, respectively. Concentrations gradually decreased to 6 and 4.3 mg/L and generally remained around this level until the conclusion of the experiment on day

212   127 in the ONMZ and ONMS systems, respectively. However, the control system maintained a

213   hypoxic condition with DO declining to 1 mg/L at day 20 of the experiment, and remaining around

214   this level throughout the tested period of 127 days. Significant differences of DO concentrations in

215   the overlaying water between each system were observed ($P<0.05$) and followed the order of ONMZ >

216   ONMS > control (**Error! Reference source not found.**3a). ORP values showed a similar pattern as

217   DO with significantly higher values in ONMZ, followed by ONMS and control systems along the

218   experiment (**Error! Reference source not found.**3b). ORP values were increased from -200 mV to

219   210 and 180 mV in the ONMZ and ONMS systems, respectively, in the first 5 days. During the

220   experiment, ORP decreased until day 20 and remained reasonably stable at 150 mV and -160 mV in

221   the ONMZ and ONMS columns, respectively, until day 89. In the control columns, the ORP showed

222   a continuous decrease from -200 mV to -350 mV by day 89.

223   **3.3 Nutrient dynamics in bottom water**

224   After 19 days of the experimental set-up, the turbidity of the overlying waters had decreased

225   from 40 NTU to around 5 NTU in the control columns and < 1 NTU in ONMZ and ONMS treated

226   systems (**Error! Reference source not found.**4a). Turbidity remained around this level until day 89.

227   The control systems had elevated TP until day 50 and significantly higher TP concentrations (0.08

228   mg/L) in the overlying water compared with the ONMZ and ONMS treated systems (Fig. 4b). The

229   TP concentrations in the ONMZ and ONMS treated columns maintained below 0.02 mg/L and did

230   not show significant differences between the two treatments.

231   TN concentrations in the ONMS columns increased slightly and the values (around 2 mg/L)

232   become significantly higher than those in ONMZ columns (around 1.5 mg/L) and in the control

233   columns (around 1.2 mg/L) at day 89 (**Error! Reference source not found.**4c). NH_4^+-N

234   concentrations showed a similar tendency of increase from day 19, with the highest concentration at

235   day 40; concentrations were around 0.1, 0.3 and 0.65 mg/L in ONMZ, ONMS and control systems,

236   respectively (**Error! Reference source not found.**4d). Concentrations of NH_4^+-N gradually

237   decreased to <0.02, 0.18 and 0.13 mg/L by day 89 in ONMZ, ONMS and control systems, respectively.

238   The concentrations of NO_3^--N (**Error! Reference source not found.**5e) and NO_2^--N (**Error!**

239   **Reference source not found.**4f) were significantly higher in the ONMZ and ONMS systems than

240   that in control after 19 days of incubation. However, the concentrations in ONMZ and ONMS systems

241   showed a clear decreasing tendency after day 80 and became similar to levels in the control systems

242   (0.01 mg/L of NO_3^--N and 0.03 mg/L of NO_2^--N).

243   **3.4 Nutrients fluxes across the sediment-water interfaces**

244   Fig. 5 shows the nutrient (TP, TN, NH_4^+-N, NO_3^--N, and NO_2^--N) fluxes across from the

245   sediment to the overlying water (effluxes) from day 26 calculated by Equation (1). The flux of TP

246   were negative in ONMZ and ONMS systems (-0.1 to -2.3 mg/m^2/d). The control system had positive

247   values of TP flux, with a decreasing tendency through time and around 0.3 mg/m^2/d at day 89 (**Error!**

248   **Reference source not found.**5a).

249   Generally, flux of TN was negative (average of -10 mg/m^2/d) in the control during the

250   experiment (**Error! Reference source not found.**5b), while values in the ONMZ systems were

251   generally positive (average of 5 mg/m^2/d). In ONMS systems, TN flux reversed from negative to

252   positive at day 47 and finally reached around 0 at day 89. The NH_4^+-N flux was positive (5-20

253   mg/m^2/d) in all systems (**Error! Reference source not found.**5c) at day 26, however, the values

declined with time, and reached around 3 mg/m^2/d in the control system and -1 and -4 mg/m^2/d in the

ONMZ and ONMS systems at day 89. **Error! Reference source not found.**5d shows that the flux of

NO$_3^-$-N in the ONMZ and ONMS systems was consistently positive (4-15 mg/m^2/d). However, the

flux of NO$_3^-$-N in the control systems was always negative (< -0.8mg/m^2/d). The flux of NO$_2^-$-N was

around 0 in the control system, however, values reversed from positive to negative in the ONMZ and

ONMS systems at day 89 (**Error! Reference source not found.**5e).

3.5 Environmental factors identified with statistical analysis

Water quality parameters (DO, ORP and turbidity) and nutrient concentrations (TP, TN, NH$_4^+$-

N, NO$_3^-$-N and NO$_2^-$-N) in the overlying water were analysed with principal component analysis

(PCA) to examine differences between treatment systems (control, ONMZ and ONMS) and sampling

times from day 19 to day 89 (**Error! Reference source not found.**6). The eigenvalues of all the

components of the PCA are shown in Table S1. The first two components (PC 1 and PC 2) contribute

high proportions (57.6% and 17.7%) of the variance in both experimental phases, thus, they were

extracted as principal components for further analysis. Clear group differences between three systems

were shown in the visualized figures (**Error! Reference source not found.**6), suggesting

performances differed by treatment. The control systems tended to locate to the left side of the

ordination, and the ONMS and ONMZ systems located in the upper right lower right side, respectively.

TP and turbidity contribute substantially to the control system performance patterns due to higher

levels of TP and turbidity in overlying water of the control systems. DO and ORP contribute more to

the positive side of PC1 (the location of the ONMS and ONMZ systems), which means the oxygen

nanobubble modified particle application reduced hypoxia/anoxia at the SWI. The DO, ORP and NO$_3^-$

-N loading factors were higher for the ONMZ than the ONMS system but this was reversed for TN,

276   NH_4^+-N and NO_2^--N.

277   Multiple correlation analysis was carried out as a blind test by homogenizing all the data from

278   all columns to assess the relationships between all the parameters (Table 1). The DO and ORP showed

279   a significant negative correlation with TP concentrations and significant positive correlation with

280   NO_3^--N concentrations. TP concentrations were also negatively correlated with TN and positively

281   correlated with turbidity.

282   **4. Discussion**

283   **4.1 Instant increase of DO by oxygen nanobubble delivery**

284   Bottom water oxygenation is an increasingly common lake management strategy for mitigating

285   hypoxia/anoxia and associated deleterious effects on water quality in deep lakes and reservoirs

286   (Bierlein et al., 2017). The current methods may require a number of large pumps with very high

287   costs and energy consumption (Funkey et al., 2014; Stigebrandt and Gustafsson, 2007). In the present

288   study, surface oxygen nanobubble technology was demonstrated to deliver oxygen into the water or

289   to the SWI using a carrier of modified zeolite (ONMZ) or soils (ONMS) through gravity settling with

290   minimum energy consumption. During the ONMZ and ONMS treatments, part of the oxygen loaded

291   on the microporous surfaces of zeolite and soil quickly diffused into water through both visible

292   microbubbles (Fig. S3) and non-visible oxygen nanobubbles (Fig. 1 and 2), and instantly increased

293   the DO concentrations from 4 mg/L to 7.5 and 5.5 mg/L in ONMZ and ONMS treated systems,

294   respectively, in the first 5 days (**Error! Reference source not found.**3a). Oxygen nanobubbles were

295   directly detected in the water through the flask experiment, which verified that they could be

296   generated/delivered and then released to the surrounding bulk water from the ONMZ and ONMS

297 (**Error! Reference source not found.**. 1 and 2). The formed oxygen-locking sediment capping layer

298 not only released oxygen into the water, but also retained oxygen which could significantly mitigate

299 and even reverse the anoxic condition at the sediment-water interfaces (Fig. 3b). Currently,

300 hypolimnetic oxygenation need to develop some novel oxygen diffuser equipment in order to prevent

301 any sediment resuspension (Gafsi et al., 2016). The settling delivery method via clay or soil particle

302 carriers can fundamentally avoid the typical problems of resuspension of sediment and rigorous

303 turbulence to the SWI faced by conventional deep water aeration methods, which may be important

304 for lake restoration in maintaining natural stratification conditions (Beutel and Horne, 1999; Gachter

305 and Wehrli, 1998). The ONMZ was more efficient in supplying oxygen to the SWI than the ONMS,

306 which may due to the locking ability of oxygen by zeolite particles as well as its larger

307 specific surface area than the natural local soils (Table S2).

308 **4.2 Sustained reversal of hypoxia/anoxia at the SWI**

309 The enhanced DO levels in bottom water resulting from oxygenation by conventional pumping

310 methods may be rapidly negated after turning the pump off (Bierlein et al., 2017; Bryant et al., 2010;

311 Gachter and Wehrli, 1998). Rapid depletion of DO occurs through oxidation of both organic detritus

312 and reduced chemical substances from the sediment and thus restoration of oxygenation is a long-

313 lasting project (Liboriussen et al., 2009). The maintenance of higher DO levels in the ONMZ and

314 ONMS treated systems in the present study can be attributed to the long lifespan of the oxygen

315 nanobubbles and oxygen retention within the capping layer. It was reported that when aerated bubbles

316 are in nano size (<200 nm), they can have much longer life than the macro bubbles (Ebina et al.,

317 2013). These oxygen nanobubbles can slowly diffuse oxygen into the water column and maintain the

318 higher DO level (4-7.5 mg/L) in ONMZ and ONMS. The reversed ORP values from -200 mV to 180-

319 210 mV in ONMZ for 89 days indicated that oxidation status can be sustained in the capping layer

320 for very long time beyond months. Part of oxygen nanobubbles can be generated and stable exist at

321 the zeolite/soil particle-water interfaces in the experiment which can be inferred from the evidence

322 that a stable cloud of O_2 nanobubbles could be found at the diatomite particle-water interface after

323 oxygen loading (Pan et al., 2016). Oxygen retention in the capping layer and downward penetration

324 of oxygen into the deeper sediment formed an oxygen-locking sediment layer and contribute to a

325 persistent reversal of anoxic condition. The oxygen nanobubbles appeared to either be active or have

326 provided sufficient oxidation to maintain elevated levels of DO and redox potential for 3-4 months in

327 the present study. At the end of present study, it was visually evidenced that around 4 cm of sediment

328 at the SWI showed a light yellow color in the ONMZ systems, which was in sharp contrast to an

329 unchanged black anoxic layer in the control systems (Fig. 7).

330 Although the previous study shows that the chitosan modified soils could form a capping layer

331 on the sediment to decrease the internal nutrients loading, the capper layer could not provide extra

332 oxygen delivery into the water and sediment and thus only can remediate the hypoxia for a short

333 period (Pan et al., 2012).The color difference of the sediment in the present study indicated that in

334 addition to direct diffusion of oxygen into the water column, there was significant amount of oxygen

335 loaded in ONMZ and ONMS that can penetrate into the sediment at a considerable depth. This likely

336 facilitated oxidation of organic matter as well as reduced substances. What is most important is that

337 such a layer provides physical isolation to prevent reduced substances from the anoxic layer from

338 diffusing upwards into the water column. Most hypoxia is formed when DO in bottom water is

339 consumed by the anaerobic substances from the sediment while there is not enough oxygen

340 replenishing from the surface water. The reversal of ORP at SWI in the ONMZ and ONMS systems

341   (Fig. 3b) could be expected to lead to oxidation of reduced forms of iron, manganese, methyl-mercury

342   and sulfide that would otherwise be released from the sediment (Beutel et al., 2008; De Vittor et al.,

343   2016; Gantzer et al., 2009; Testa and Kemp, 2012; Zhu et al., 2013). The nanobubble technology

344   demonstrated in this study appeared to provide a novel principle for the remediation of

345   hypoxia/anoxia in the bottom water.

346   **4.3 Manipulating nutrients fluxes at SWI**

347   Reversal of hypoxia/anoxia may not only prevent the release of reduced species release and

348   facilitate organic matter mineralization (Beutel et al., 2008; De Vittor et al., 2016; Gantzer et al., 2009;

349   Testa and Kemp, 2012), but can also influence nutrient recycling across SWI. In the present study,

350   evidence of the positive effect of alleviation of hypoxia remediation on nutrient recycling was found

351   in the significant differences in nutrient concentrations and fluxes across SWI between the ONMZ

352   and ONMS treated and control systems (**Error! Reference source not found.**4 and **Error!**

353   **Reference source not found.**5). Obvious P release from the sediment to the overlying water occurred

354   in the control system, however, there was a net flux of TP from water to the sediments in the ONMZ

355   and ONMS systems (**Error! Reference source not found.**4b and **Error! Reference source not**

356   **found.**5a). Although, in some previous reports, capping with unmodified materials could also

357   influence nutrient fluxes in short period (Faithfull et al., 2008; Pan et al., 2012), no evidence showed

358   these materials could reversal the sediment hypoxia/anoxia which can contribute to P fixation in

359   sediment. The main mechanism of the P release from sediments is generally related to changes in

360   redox-sensitive iron and manganese oxide minerals and the associated P (Funes et al., 2016; Jordan

361   et al., 2008), with inorganic phosphorus generally adsorbed by the metal oxide–hydroxide complexes

362   under oxic conditions (Tang et al., 2013; Xu et al., 2013). Reversal of the ORP sign (i.e., positive

363   values) in ONMZ treated systems indicated that the SWI changed from anoxic to oxic. Jilbert et al.

364   (2011) found preferential remineralization of P in relation to carbon and nitrogen during

365   decomposition of organic substances induced by reducing conditions plays a key role leading to

366   surplus bioavailable P in the Baltic Sea, and was likely why TP concentrations in the overlying water

367   were significantly positively correlated with DO and ORP (Table 1). Reversal of ORP in ONMZ

368   induced a conversion of sediment from P sources to sinks compared with that in the control.

369   Changes in redox potential affect N transformations from bacterial activities at the SWI,

370   particularly nitrification, denitrification and anammox reactions (Brzozowska and Gawronska, 2009).

371   The significantly higher oxygen condition induced by surface oxygen nanobubble materials (**Error!**

372   **Reference source not found.**3) may facilitate nitrification, which converts NH_4^+-N to NO_3^--N

373   (Rassamee et al., 2011). Thus, lower NH_4^+-N occurred in ONMZ. Moreover, nitrification can supply

374   necessary NO_2^--N as an electron acceptor to anammox bacteria which can reduce NH_4^+-N to nitrogen

375   gas (Kim et al., 2016). Nitrification-anammox coupling reactions often occur between aerobic and

376   anaerobic zones (Brzozowska and Gawronska, 2009), notably in the SWI region. The co-existence

377   of nitrification and anammox in the treated systems may reduce the efflux of NH_4^+-N in the

378   experimental systems compared with those in the control at the end of the experiment (**Error!**

379   **Reference source not found.**5c). In control systems, anaerobic conditions not only hinder

380   nitrification and supply of NO_2^--N for anammox bacteria but may also stimulate sulfide accumulation,

381   further inhibiting nitrification (Jensen et al., 2008). Thus, the lowest concentrations of NO_3^--N in the

382   control systems were likely to have been through denitrification (**Error! Reference source not**

383   **found.**4e). Beyond denitrification, dissimilatory NO_3^--N reduction to NH_4^+-N can also be facilitated

384   under anoxic conditions (McCarthy et al., 2008). The sum of these effects contributed to the reduced

385 TN efflux in the treated systems (**Error! Reference source not found.**5b). It should be noted that

386 local soils, collected from the lake and used in our experiment, may contain more organic matter than

387 zeolite. The higher NH_4^+-N concentrations in the ONMS treated systems might be produced by

388 mineralization of organic N from the soils (**Error! Reference source not found.**4d). Previous studies

389 point out that organic matter in the anoxic sediment could be degraded together with N

390 transformations from organic N to NH_4^+-N within two weeks (Han et al., 2015; Xu et al., 2013). This

391 is consistent with our results that NH_4^+-N increased between 19 and 33 days and decreased in the

392 subsequent days in all the three systems (**Error! Reference source not found.**4d). As a result of

393 these processes above mentioned, using surface oxygen nanobubble technology can significantly

394 regulate the biogeochemical processes that regulate species of phosphorus and nitrogen at the SWI.

395 It would be an important topic to study the role of oxygen nanobubbles in relation to microbial

396 communities under controlled laboratory and field conditions.

397 **4.4 Implementation perspective for lake geo-engineering**

398 The present study has, for the first time, indicated that oxygen nanobubble modified clays can

399 deliver amounts of oxygen into both water and sediment where there has previously been

400 hypoxia/anoxia. By using the geo-engineering method developed based on oxygen nanobubbles, it is

401 possible to deliver oxygen into bottom water/sediment through gravity settling, which can achieve

402 both replenishing oxygen consumption in the "dead zone" with minimum energy consumption and

403 minimizing the disturbance to the water stratification and surface sediment. The prolonged time

404 effects of oxygen nanobubbles, denoted by improving oxygen levels and reversal of ORP, may further

405 trigger a series changes in physico-chemical and microbial responses at SWI. Nevertheless, the in-

406 site experiment of the surface nanobubble technology in lakes and sea waters need to be further

407 investigated.

5. Conclusions

409 The study verified a novel principle for combating hypoxia/anoxia at the sediment-water

410 interfaces using oxygen nanobubble technology. The synergistic effects of diffusion and retention of

411 oxygen in the nanobubble modified natural zeolite (ONMZ) and local soils (ONMS) contributed to

412 mitigating sediment anoxia and controlling phosphorus release from bottom sediments. It was found

413 that amount of oxygen loaded in clay particles could release via both macro- and nano-scale bubbles

414 and quickly increase the DO levels in water column. Moreover, the oxygen nanobubbles in the

415 modified particles could stably retain at SWI and penetrate oxygen downward to the sub-layer

416 sediment, and then form an oxygen-locking sediment layer between the anoxic sediment and water

417 column. This layer can sustainably reverse hypoxia/anoxia condition at SWI for several months.

418 Finally, nutrient fluxes across the SWI could be regulated by capping with oxygen nanobubble

419 modified materials in which the bottom sediments become adsorptive for phosphorus, rather than

420 releasing it. In this study we have demonstrated the potential for a major breakthrough in remediation

421 of aquatic systems via geo-engineering and delivery of oxygen and form oxygen-locking later into

422 the deep sediment-water interface, which is crucial for eutrophication control and ecological

423 restoration.

431

References

432

433 Agarwal A, Ng WJ, Liu Y, 2011. Principle and applications of microbubble and nanobubble

434   technology for water treatment. Chemosphere 84 (9), 1175-1180.

435 APHA, 1998. Standard methods for the examination of water and wastewat. American Public Health

436   Association, Washington DC 20th Edition.

437 Beutel MW, Horne AJ, 1999. A Review of the Effects of Hypolimnetic Oxygenation on Lake and

438   Reservoir Water Quality. Lake Reservoir Manag. 15 (4), 285-297.

439 Beutel MW, Leonard TM, Dent SR, Moore BC, 2008. Effects of aerobic and anaerobic conditions on

440   P, N, Fe, Mn, and Hg accumulation in waters overlaying profundal sediments of an oligo-

441   mesotrophic lake. Water Res. 42 (8-9), 1953-1962.

442 Bierlein KA, Rezvani M, Socolofsky SA, Bryant LD, Wüest A, Little JC, 2017. Increased sediment

443   oxygen flux in lakes and reservoirs: The impact of hypolimnetic oxygenation. Water Resources

444   Research.

445 Bormans M, Marsalek B, Jancula D, 2016. Controlling internal phosphorus loading in lakes by

446   physical methods to reduce cyanobacterial blooms: a review. Aquat. Ecol. 50 (3), 407-422.

447 Bryant LD, Lorrai C, McGinnis DF, Brand A, Wuest A, Little JC, 2010. Variable sediment oxygen

448   uptake in response to dynamic forcing. Limnol. Oceanogr. 55 (2), 950-964.

449 Brzozowska R, Gawronska H, 2009. The influence of a long-term artificial aeration on the nitrogen

450   compounds exchange between bottom sediments and water in Lake Dlugie. Oceanological and

451   Hydrobiological Studies 38 (1), 113-119.

452 Cai WB, Yang HL, Zhang J, Yin JK, Yang YL, Yuan LJ, et al., 2015. The Optimized Fabrication of

453   Nanobubbles as Ultrasound Contrast Agents for Tumor Imaging. Sci Rep-Uk 5, 13725.

454   Carstensen J, Andersen JH, Gustafsson BG, Conley DJ, 2014. Deoxygenation of the Baltic Sea during

455   the last century. Proc. Natl. Acad. Sci. U. S. A. 111 (15), 5628-5633.

456   Cavalli R, Bisazza A, Rolfo A, Balbis S, Madonnaripa D, Caniggia I, et al., 2009. Ultrasound-

457   mediated oxygen delivery from chitosan nanobubbles. Int. J. Pharm. 378 (1–2), 215-217.

458   Conley DJ, Bonsdorff E, Carstensen J, Destouni G, Gustafsson BG, Hansson LA, et al., 2009.

459   Tackling Hypoxia in the Baltic Sea: Is Engineering a Solution? Environ. Sci. Technol. 43 (10),

460   3407-3411.

461   De Vittor C, Relitti F, Kralj M, Covelli S, Emili A, 2016. Oxygen, carbon, and nutrient exchanges at

462   the sediment–water interface in the Mar Piccolo of Taranto (Ionian Sea, southern Italy). Environ.

463   Sci. Pollut. Res. 23 (13), 12566-12581.

464   Diaz RJ, Rosenberg R, 2008. Spreading dead zones and consequences for marine ecosystems. Science

465   321 (5891), 926-929.

466   Ebina K, Shi K, Hirao M, Hashimoto J, Kawato Y, Kaneshiro S, et al., 2013. Oxygen and Air

467   Nanobubble Water Solution Promote the Growth of Plants, Fishes, and Mice. PLoS One 8 (6).

468   Faithfull CL, Hamilton DP, Burger DF, Duggan IC. Waikato peat lakes sediment nutrient removal

469   scoping exercise. CBER Contract Report. The University of Waikato, 2008.

470   Feist TJ, Pauer JJ, Melendez W, Lehrter JC, DePetro PA, Rygwelski KR, et al., 2016. Modeling the

471   Relative Importance of Nutrient and Carbon Loads, Boundary Fluxes, and Sediment Fluxes on

472   Gulf of Mexico Hypoxia. Environ. Sci. Technol. 50 (16), 8713-8721.

473   Forth M, Liljebladh B, Stigebrandt A, Hall POJ, Treusch AH, 2015. Effects of ecological engineered

474   oxygenation on the bacterial community structure in an anoxic fjord in western Sweden. ISME J.

475   9 (3), 656-669.

476   Funes A, de Vicente J, Cruz-Pizarro L, Alvarez-Manzaneda I, de Vicente I, 2016. Magnetic

477   microparticles as a new tool for lake restoration: A microcosm experiment for evaluating the

478   impact on phosphorus fluxes and sedimentary phosphorus pools. Water Res. 89, 366-374.

479   Funkey CP, Conley DJ, Reuss NS, Humborg C, Jilbert T, Slomp CP, 2014. Hypoxia Sustains

480   Cyanobacteria Blooms in the Baltic Sea. Environ. Sci. Technol. 48 (5), 2598-2602.

481   Gachter R, Wehrli B, 1998. Ten years of artificial mixing and oxygenation: No effect on the internal

482   phosphorus loading of two eutrophic lakes. Environ. Sci. Technol. 32 (23), 3659-3665.

483   Gafsi M, Kettab A, Djehiche A, Goteicha K, 2016. Study of the efficiency of hypolimnetic aeration

484   process on the preservation of the thermal stratification. Desalin Water Treat 57 (13), 6017-6023.

485   Gantzer PA, Bryant LD, Little JC, 2009. Controlling soluble iron and manganese in a water-supply

486   reservoir using hypolimnetic oxygenation. Water Res. 43 (5), 1285-1294.

487   Han C, Ding SM, Yao L, Shen QS, Zhu CG, Wang Y, et al., 2015. Dynamics of phosphorus-iron-

488   sulfur at the sediment-water interface influenced by algae blooms decomposition. J. Hazard.

489   Mater. 300, 329-337.

490   Henares MNP, Preto BD, Rosa FRT, Valenti WC, Camargo AFM, 2015. Effects of artificial substrate

491   and night-time aeration on the water quality in Macrobrachium amazonicum (Heller 1862) pond

492   culture. Aquac. Res. 46 (3), 618-625.

493   Huser BJ, Futter M, Lee JT, Perniel M, 2016. In-lake measures for phosphorus control: The most

494   feasible and cost-effective solution for long-term management of water quality in urban lakes.

495   Water Res. 97, 142-152.

496   Jensen MM, Kuypers MMM, Lavik G, Thamdrup B, 2008. Rates and regulation of anaerobic

497   ammonium oxidation and denitrification in the Black Sea. Limnol. Oceanogr. 53 (1), 23-36.

498   Jilbert T, Slomp CP, Gustafsson BG, Boer W, 2011. Beyond the Fe-P-redox connection: preferential

499   regeneration of phosphorus from organic matter as a key control on Baltic Sea nutrient cycles.

500   Biogeosciences 8 (6), 1699-1720.

501   Jordan TE, Cornwell JC, Boynton WR, Anderson JT, 2008. Changes in phosphorus biogeochemistry

502   along an estuarine salinity gradient: The iron conveyer belt. Limnol. Oceanogr. 53 (1), 172-184.

503   Kim H, Ogram A, Bae H-S, 2016. Nitrification, Anammox and Denitrification along a Nutrient

504   Gradient in the Florida Everglades. Wetlands, 1-9.

505   Li L, Pan G, 2013. A universal method for flocculating harmful algal blooms in marine and fresh

506   waters using modified sand. Environ. Sci. Technol. 47 (9), 4555-4562.

507   Liboriussen L, Sondergaard M, Jeppesen E, Thorsgaard I, Grunfeld S, Jakobsen TS, et al., 2009.

508   Effects of hypolimnetic oxygenation on water quality: results from five Danish lakes.

509   Hydrobiologia 625, 157-172.

510   McCarthy MJ, McNeal KS, Morse JW, Gardner WS, 2008. Bottom-water hypoxia effects on

511   sediment-water interface nitrogen transformations in a seasonally hypoxic, shallow bay (Corpus

512   christi bay, TX, USA). Estuaries and Coasts 31 (3), 521-531.

513   Noyma NP, de Magalhães L, Furtado LL, Mucci M, van Oosterhout F, Huszar VLM, et al., 2016.

514   Controlling cyanobacterial blooms through effective flocculation and sedimentation with

515   combined use of flocculants and phosphorus adsorbing natural soil and modified clay. Water Res.

516   97, 26-38.

517   Pan G, Dai LC, Li L, He LC, Li H, Bi L, et al., 2012. Reducing the Recruitment of Sedimented Algae

518   and Nutrient Release into the Overlying Water Using Modified Soil/Sand Flocculation-Capping

519   in Eutrophic Lakes. Environ. Sci. Technol. 46 (9), 5077-5084.

520 Pan G, He G, Zhang M, Zhou Q, Tyliszczak T, Tai R, et al., 2016. Nanobubbles at Hydrophilic

521   Particle-Water Interfaces. Langmuir 32 (43), 11133-11137.

522 Pan G, Krom MD, Zhang MY, Zhang XW, Wang LJ, Dai LC, et al., 2013. Impact of Suspended

523   Inorganic Particles on Phosphorus Cycling in the Yellow River (China). Environ. Sci. Technol.

524   47 (17), 9685-9692.

525 Pan G, Yang B, 2012. Effect of Surface Hydrophobicity on the Formation and Stability of Oxygen

526   Nanobubbles. Chemphyschem 13 (8), 2205-2212.

527 Pan G, Yang B, Lei L, Lei, Liao L, Ding C, Wang D, 2011. A method for remediating of anoxic

528   sediment in lakes by using nanobubbles. Patent NO. 200910080563.5.

529 Peng H, Birkett GR, Nguyen AV, 2015. Progress on the Surface Nanobubble Story: What is in the

530   bubble? Why does it exist? Adv. Colloid Interface Sci. 222, 573-580.

531 Rassamee V, Sattayatewa C, Pagilla K, Chandran K, 2011. Effect of Oxic and Anoxic Conditions on

532   Nitrous Oxide Emissions from Nitrification and Denitrification Processes. Biotechnol. Bioeng.

533   108 (9), 2036-2045.

534 Spears BM, Maberly SC, Pan G, Mackay E, Bruere A, Corker N, et al., 2014. Geo-Engineering in

535   Lakes: A Crisis of Confidence? Environ. Sci. Technol. 48 (17), 9977-9979.

536 Stigebrandt A, Gustafsson BG, 2007. Improvement of Baltic proper water quality using large-scale

537   ecological engineering. Ambio 36 (2-3), 280-286.

538 Stramma L, Johnson GC, Sprintall J, Mohrholz V, 2008. Expanding oxygen-minimum zones in the

539   tropical oceans. Science 320 (5876), 655-658.

540 Tang WZ, Zhang H, Zhang WQ, Wang C, Shan BQ, 2013. Biological invasions induced phosphorus

541   release from sediments in freshwater ecosystems. Colloid Surface A 436, 873-880.

542 Testa JM, Kemp WM, 2012. Hypoxia-induced shifts in nitrogen and phosphorus cycling in

543   Chesapeake Bay. Limnol. Oceanogr. 57 (3), 835-850.

544 Waajen G, van Oosterhout F, Douglas G, Lürling M, 2016. Geo-engineering experiments in two

545   urban ponds to control eutrophication. Water Res. 97, 69-82.

546 Wang L, Miao XJ, Pan G, 2016. Microwave-Induced Interfacial Nanobubbles. Langmuir 32 (43),

547   11147-11154.

548 Xu D, Chen YF, Ding SM, Sun Q, Wang Y, Zhang CS, 2013. Diffusive Gradients in Thin Films

549   Technique Equipped with a Mixed Binding Gel for Simultaneous Measurements of Dissolved

550   Reactive Phosphorus and Dissolved Iron. Environ. Sci. Technol. 47 (18), 10477-10484.

551 Yang CW, Lu YH, Hwang IS, 2013. Condensation of Dissolved Gas Molecules at a

552   Hydrophobic/Water Interface. Chinese J Phys 51 (1), 174-186.

553 Zhang ZS, Wang G, Li Y, Zhang X, Qiao NL, Wang JH, et al., 2014. A new type of ordered

554   mesoporous carbon/polyaniline composites prepared by a two-step nanocasting method for high

555   performance supercapacitor applications. J Mater Chem A 2 (39), 16715-16722.

556 Zhu G, Wang S, Wang W, Wang Y, Zhou L, Jiang B, et al., 2013. Hotspots of anaerobic ammonium

557   oxidation at land-freshwater interfaces. Nature Geosci 6 (2), 103-107.

558

559

560